

## **Down-regulation of respiration in pear fruit depends on temperature**

*Q. T. Ho, M.L.A.T.M. Hertog, P. Verboven, A. Ambaw, S. Rogge, B. E. Verlinden and B. M. Nicolai*

### **SUPPLEMENTARY DATA**

**Protocol S1.** Modelling the response of  $V_{m,O_2}$  to  $O_2$  level

**Protocol S2.** Temperature dependency of respiration capacity

**Protocol S3.** Amplitude of regulation of maximal respiration rate by  $O_2$

**Protocol S4.** Criterion for goodness of fit of the model

**Protocol S5.** Heat conduction model

**Table S1.** Description of data sets used in calibration and validation of model

**Figure S1.** Proposed reactions and modelled equations describing response of receptor, enzyme and respiration to  $O_2$  level.

**Figure S2.**  $O_2$  consumption rate of intact pear fruit as a function of time at 20 kPa  $O_2$ , 0 kPa  $CO_2$  at 10 °C.

**Figure S3.**  $O_2$  consumption rate of intact pear fruit as a function of time during storage of fruit at 20 kPa  $O_2$ , 0 kPa  $CO_2$  at 0 °C.

**Figure S4.** Dynamic response of  $O_2$  consumption rate ( $R_{O_2}$ ) to  $O_2$  level and time at 0 °C (experiment B).

**Figure S5.** Response of  $R_{O_2}$  of intact pear fruit to  $O_2$  (A) and time (B) (experiment C).

**Figure S6.** (A) Steady state modelled response of relative maximal  $O_2$  consumption rate to  $O_2$  level. (B) Change of maximal  $O_2$  consumption rate in response to a sudden drop of the  $O_2$  concentration.

**Figure S7.** Comparison of fitting between the adapted respiration model ( $m = 2$ ) and the respiration model with assumption of variation of  $K_{m,O_2}$  at 0 °C.

**Figure S8.** Comparison of fitting between the adapted respiration model ( $m = 2$ ) and the respiration model with assumption of variation of  $K_{m,O_2}$  at 0 °C.

**Figure S9.** Respiration rate of intact pear fruit as a function of the  $O_2$  concentration at 20 °C (A, B), 10 °C (C, D), and 5 °C (E, F) harvested in season 2016.

**Figure S10.** Predicted temperature of pear fruit during cooling.

**Figure S11.** Simulations with a two-compartment model (core and cortex) and different combinations of diffusivities and  $V_{max}$  values.

**Figure S12.** Steady state modelled response of relative maximal O<sub>2</sub> consumption rate ( $V_{m,O_2} / \max(V_{m,O_2})$ ) to O<sub>2</sub> level.

**Figure S13.** Simulated  $V_{m,O_2}$  of pear fruit in the closed jar at 20 °C (I), 10 °C (II) and 0 °C (III) and different times.

**Figure S14.** Simulated O<sub>2</sub> and CO<sub>2</sub> gas partial pressure profiles from the center to the surface along the radial direction in the closed jar at 20 °C (I), 10 °C (II) and 0 °C (III) at different times.

### Protocol S1. Modelling the response of $V_{m,O_2}$ to $O_2$ level

We assumed that a receptor in a pear cell can be activated by  $O_2$ , causing a signal transduction cascade that results in a final change in enzyme concentrations involved in respiration (Fig. S1). Change of activation of the receptor by  $O_2$  which is assumed to be described by the Hill equation (reaction R1, Fig. S1) could be written as

$$\frac{\partial [R_a]}{\partial t} = k_{H1} \cdot [R] \cdot [O_2]^m - (k_{H2} + k_{d2}) \cdot [R_a] \quad (S1)$$

where  $[O_2]$  is the  $O_2$  concentration;  $[R_a]$  and  $[R]$  are the concentrations of active and inactive receptors, respectively;  $m$  is the number of  $O_2$  molecules aggregating one receptor molecule,  $k_{H1}$  and  $k_{H2}$  are the rate constants of the Hill equation;  $k_{d2}$  is the rate constant of receptor degradation;  $t$  (s) is time. Note that if  $m = 1$ , the Hill equation becomes a Michaelis Menten kinetics. If  $m > 1$ , then the binding of  $O_2$  to the receptor causes the affinity for other  $O_2$  molecules to increase.

Here, the activate receptor is assumed to trigger a biochemical chain involving in transcription and translation steps, resulting the final level of the enzyme  $E$ . Since quantitative kinetic parameters of the transcription and translation is unavailable, we simply assumed that change in level of the enzyme  $E$  in response to the activate receptor was characterized by a lumped synthesis rate  $k_s$  agglomerating multiple conversion steps in a signal transduction cascade. Such response of enzyme and/or protein to signal has been described by simple reaction (Tchourine *et al.*, 2014). The corresponding change of enzyme concentration  $E$  in response to level of the receptor is assumed as:

$$\frac{\partial [E]}{\partial t} = k_s \cdot [R_a] \cdot [AA] - k_d \cdot [E] \quad (S2)$$

where  $[E]$  is the concentration of enzyme initially available;  $k_s$  represents the overall rate constant of enzyme synthesis taking into account transcription and translation;  $k_d$  is the rate constant of enzyme degradation;  $[AA]$  is the amount of amino acid involving in enzyme synthesis (assumed to be constant).

Respiration has been commonly described by an existing Michaelis Menten kinetics (Hertog *et al.*, 1998). In this study, we assumed that the response of the maximal respiration rate  $V_{m,O_2}$  was proportional to the change of enzymes involving in the respiration

$$\frac{\partial V_{m,O_2}}{\partial t} = k_p \frac{\partial [E]}{\partial t} \quad (S3)$$

Where  $k_p$  is the reaction rate constant for the formation of CO<sub>2</sub> product (Hertog *et al.*, 1998).

The Eq. (S3) can be approximated as

$$V_{m,O_2} = k_p \cdot [E] + V_{R,1} \quad (S4)$$

Solving Eq. (S4) for  $[E]$ , substituting into Eq. (S2) yields:

$$\frac{\partial V_{m,O_2}}{\partial t} = k_p \cdot k_s \cdot [R_a] \cdot [AA] - k_d \cdot V_{m,O_2} + k_d \cdot V_{R,1} \quad (S5)$$

Activation of the signal can be considered at a quasi-steady state; hence Eq. (S1) is assumed to equal to zero and together with equation (S5) rearranged to obtain an expression for  $V_{m,O_2}$ :

$$\frac{\partial V_{m,O_2}}{\partial t} = k_d \cdot (V_R - V_{m,O_2}) \quad (S6)$$

$$V_R = V_{R,1} + \frac{(V_{R,2} - V_{R,1}) \cdot [O_2]^m}{K_H + [O_2]^m} = V_{R,1} + \frac{\Delta V \cdot [O_2]^m}{K_H + [O_2]^m} \quad (S7)$$

$$\text{with } V_{R,2} = V_{R,1} + \frac{k_p \cdot k_s \cdot [R_T] \cdot [AA]}{k_d} \quad (S8); \quad K_H = \frac{k_{H2} + k_{d2}}{k_{H1}} \quad (S9);$$

$$[R_T] = [R_a] + [R] \quad (S10); \quad \Delta V = \frac{k_p \cdot k_s \cdot [R_T] \cdot [AA]}{k_d} \quad (S11);$$

In Eq. (S7),  $V_{R,1}$  is a base affinity to O<sub>2</sub>;  $V_{R,2}$  is the maximal O<sub>2</sub> consumption rate in the presence of O<sub>2</sub>;  $\Delta V$  represents the amplitude of the regulation of the maximal respiration rate by O<sub>2</sub>.

## Protocol S2. Temperature dependency of respiration capacity

The effect of temperature on the maximal O<sub>2</sub> consumption rate  $V_{m,O_2}$  and the maximal fermentative CO<sub>2</sub> production rate  $V_{m,f,CO_2}$  was described by Arrhenius's law (Hertog *et al.*, 1998).

$$V_{m,O_2} = V_{m,O_2,ref} \exp \left[ \frac{E_{a,V_{m,O_2}}}{R} \left( \frac{1}{T_{ref}} - \frac{1}{T} \right) \right] \quad (S12)$$

$$V_{m,f,CO_2} = V_{m,f,CO_2,ref} \exp \left[ \frac{E_{a,V_{m,f,CO_2}}}{R} \left( \frac{1}{T_{ref}} - \frac{1}{T} \right) \right] \quad (S13)$$

where  $V_{m,O_2,ref}$  ( $\mu\text{mol m}^{-3} \text{s}^{-1}$ ) and  $V_{m,f,CO_2,ref}$  ( $\mu\text{mol m}^{-3} \text{s}^{-1}$ ) are the maximal  $O_2$  consumption rate and maximal fermentative  $CO_2$  production rate at  $T_{ref}=283\text{K}$ , respectively;  $E_{a,V_{m,O_2}}$  and  $E_{a,V_{m,f,CO_2}}$  ( $\text{kJ mol}^{-1}$ ) are the activation energies for  $O_2$  consumption and fermentative  $CO_2$  production;  $T$  (K) temperature; and  $R$  ( $8.314 \text{ J mol}^{-1} \text{ K}^{-1}$ ) the universal gas constant.

### Protocol S3. Amplitude of regulation of maximal respiration rate by $O_2$

The amplitude of regulation of maximal respiration rate by  $O_2$ ,  $\Delta V$  was derived from Eq. S11. In the equation, parameters  $k_d$  and  $k_p$  are the reaction rate constants of enzyme degradation and  $CO_2$  production rate while  $k_s$  represents the overall rate constant of enzyme production. The effect of temperature on  $\Delta V$  by both  $k_d$  and  $k_p$  was presumably cancelled in Eq. (S11) if they were assumed to have the same activation energy.  $k_s$  being the rate constant agglomerating multiple conversion steps including transcription and translation was assumed to be less affected by low temperature. Note that to response to low temperature stress, ribosomes might modify their translation machine to facilitate protein synthesis. For instance, the AOX amount (transcript, protein or capacity) has been reported to increase at low temperature (Fung *et al.*, 2004; Sugie *et al.*, 2006) although the respiration rate was considerably reduced. Our results indicated that ratio of  $\Delta V/V_{R,2}$  was rather low at high temperature as compared to low temperature. Assuming that  $\Delta V$  ranged from 0 to 0.21 fold the value of maximal respiration rate  $V_{R,2}$  at  $10\text{ }^\circ\text{C}$  and  $20\text{ }^\circ\text{C}$ , the model predictions are comparable to the measurement. In contrast, at low temperature the model prediction show a good agreement with the measurement when amplitude of the regulation of respiration was high ( $\Delta V_R$  equal to 0.66 fold the value of  $V_{R,2}$ ).

### Protocol S4. Criterion for goodness of fit of the model

$R^2$  is a statistical measure of how close the fitted model to data is. In general, the  $R^2$  is defined as:

$$R^2 = 1 - \frac{SS_{res}}{SS_{tot}} \quad (\text{S14})$$

where  $SS_{res}$  and  $SS_{tot}$  are the total sum of squares of the data and the regression sum of squares, respectively.  $SS_{res}$  and  $SS_{tot}$  are defined as:

$$SS_{res} = \sum (y_i - f_i) \quad (S15)$$

$$SS_{tot} = \sum (y_i - \bar{y}) \quad (S16)$$

where  $y_i$ ,  $\bar{y}$  and  $f_i$  are the measured data, the mean of the measured data and the predicted value by the model, respectively.

### Protocol S5. Heat conduction model

A model of heat conduction inside pear fruit was performed to predict the cooling time and temperature profile within the pear at 0 °C. Heat conduction within the pear fruit is described as follows:

$$\rho C_p \frac{\partial T}{\partial t} = \nabla \cdot k \nabla T + Q \quad (S17)$$

where  $\rho$  (~1000 kg m<sup>-3</sup>) is the fruit density,  $C_p$  (3.69 kJ kg<sup>-1</sup> K<sup>-1</sup>, Ramaswamy and Tung, 1981) is the heat capacity of the fruit tissue,  $k$  (0.427 W m<sup>-1</sup> K<sup>-1</sup>, Ramaswamy and Tung, 1981) is the heat conductivity of the fruit tissue.  $Q$  (W m<sup>-3</sup>) is the heat generation.  $Q$  can be calculated from the respiration rate as follows

$$Q = -q_{O_2} R_{O_2} \quad (S18)$$

where  $q_{O_2}$  (J mol<sup>-1</sup> O<sub>2</sub> consumed) is the proportional constant. In aerobic conditions and when glucose is the substrate,  $q_{O_2}$  has a value of 478.3 kJ mol<sup>-1</sup> O<sub>2</sub> consumed (Datta et al., 2005).

At the fruit surface the following boundary condition was assumed:

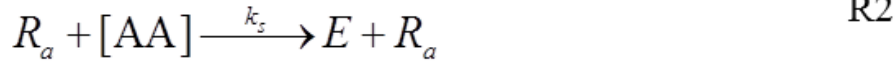
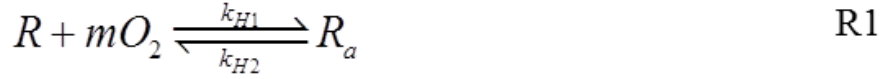
$$-k \frac{\partial T}{\partial n} = h_m (T - T_\infty) \quad (S19)$$

with  $n$  the outward normal to the surface; the index  $\infty$  referring to the ambient temperature;  $h_m$  the heat transfer coefficient (W m<sup>-2</sup> K<sup>-1</sup>). For nature convection, value of  $h_m$  is assumed to be 5 W m<sup>-2</sup> K<sup>-1</sup>.

Equations S17-S19 combined with equations (1-4) were numerically solved using the finite element method (Comsol 3.5, Comsol AB, Stockholm). Simulation results showed that the pear was completely cooled from 20 °C to 0 °C after 10 h and the temperature was homogeneous throughout the fruit (temperature difference less than 0.012 °C). (Fig. S10).

**Table S1.** Description of data sets used in calibration and validation of model

Experiment	Date	Condition	Description
A	15/10/2010, 28/10/2010, 04/11/2014, 16/11/2016, 30/11/2016, 21/12/2016	Fruit were taken from CA storage and put at normal ambient condition at 0 °C for 3 days before starting the experiment.	Determination of the maximal O <sub>2</sub> consumption rate and the maximal fermentative CO <sub>2</sub> production rate
B1 B2 B3	26/01/2015 26/01/2015 10/11/2014	Fruit were taken from CA storage and put at normal ambient condition at 0 °C for 1 day before starting the experiment.	Estimation of parameters $k_a$ , the time response of $V_{m,O_2}$ to O <sub>2</sub> level and $K_H$ the sensitivity of $V_{m,O_2}$ to O <sub>2</sub> level at 0 °C (see Fig. 4, Fig. 5).
C	21/10/2014	Fruit were taken from CA storage and put at normal ambient condition at 0 °C for 1 day before starting the experiment.	
D1	07/11/2014	Fruit were taken from CA storage and put 7 days at normal ambient condition at 0 °C before starting the experiment.	Validation at 10 °C (see Fig. 1)
D2	15/09/2014	Fruit were taken from normal ambient storage at 0 °C before starting the experiment.	Validation at 0 °C (see Fig. 1)
D3	15/10/2010	Fruit were taken from normal ambient storage at -1 °C before starting the experiment.	Validation at 20 °C (see Fig. 1). Data was published in Ho et al., (2015).
D4	28/10/2010	Fruit were taken from normal ambient storage at -1 °C before starting the experiment.	Validation at 10 °C. Data was published in Ho et al., (2015).
D5	16/11/2016	Fruit were taken from normal ambient storage at 0 °C before starting the experiment.	Validation at 20 °C (see Fig. S8).
D6	07/12/2016	Fruit were taken from normal ambient storage at 0 °C before starting the experiment.	Validation at 10 °C (see Fig. S8).
D7	16/11/2016	Fruit were taken from normal ambient storage at 0 °C before starting the experiment.	Validation at 5 °C (see Fig. S8).



$$\frac{\partial [R_a]}{\partial t} = k_{H1} \cdot [R] \cdot [O_2]^m - (k_{H2} + k_{d2}) \cdot [R_a] \quad \text{Eq1}$$

$$\frac{\partial [E]}{\partial t} = k_s \cdot [R_a] \cdot [AA] - k_d \cdot [E] \quad \text{Eq2}$$

**Fig. S1. Proposed reactions and modelled equations describing response of receptor, enzyme and respiration to O<sub>2</sub> level.** In the signal-enzyme mechanism (reaction R1), the receptor  $R$  is assumed to be activated or inhibited by O<sub>2</sub> level and described by Hill equation while the concentration of the enzyme  $E$  is controlled by the synthesis rate  $k_s$  agglomerating multiple conversion steps including transcription and translation. Eq1 and Eq2 in Fig. S1 represent time dependent concentrations of the receptor and enzyme in response to O<sub>2</sub> level. Symbols are defined in Supplementary Text S1.



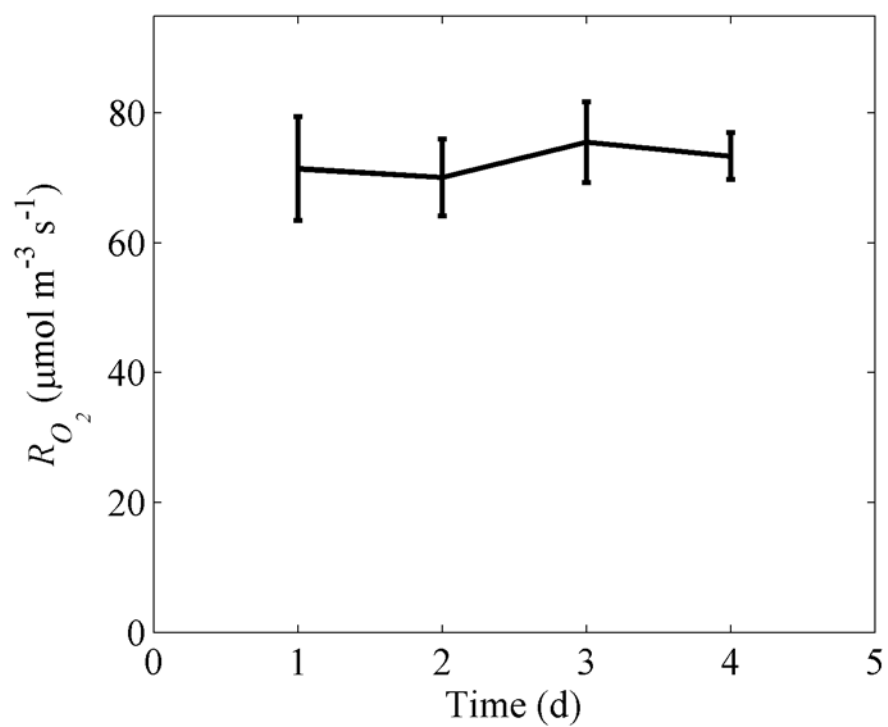


**Fig. S2.  $O_2$  consumption rate of intact pear fruit as a function of time at 20 kPa  $O_2$ , 0 kPa  $CO_2$  at 10 °C.**

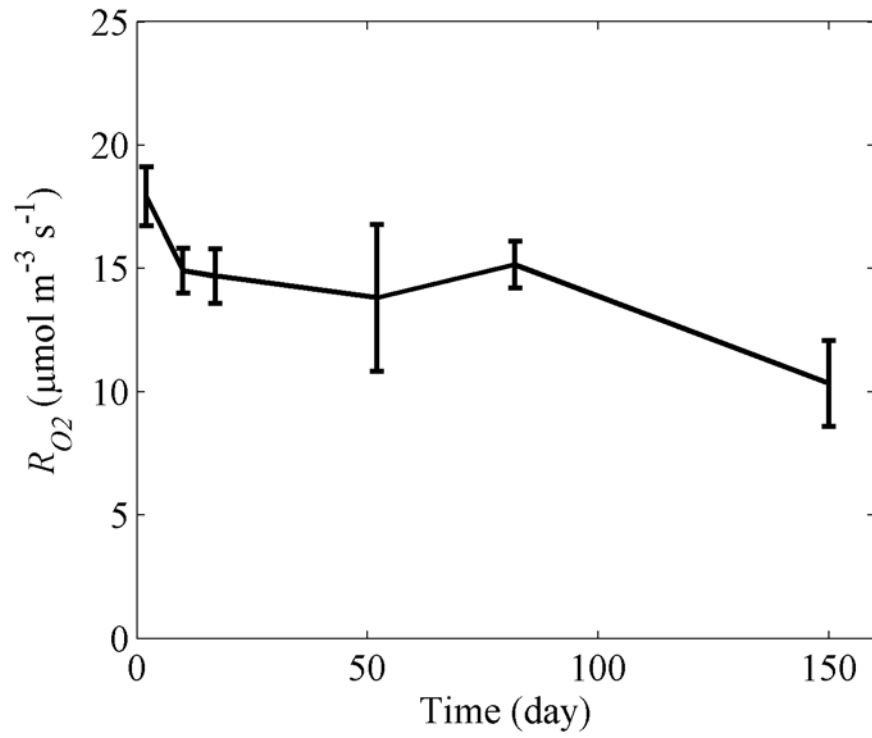


**Fig. S3.  $O_2$  consumption rate of intact pear fruit as a function of time during storage of fruit at 20 kPa  $O_2$ , 0 kPa  $CO_2$  at 0 °C.**

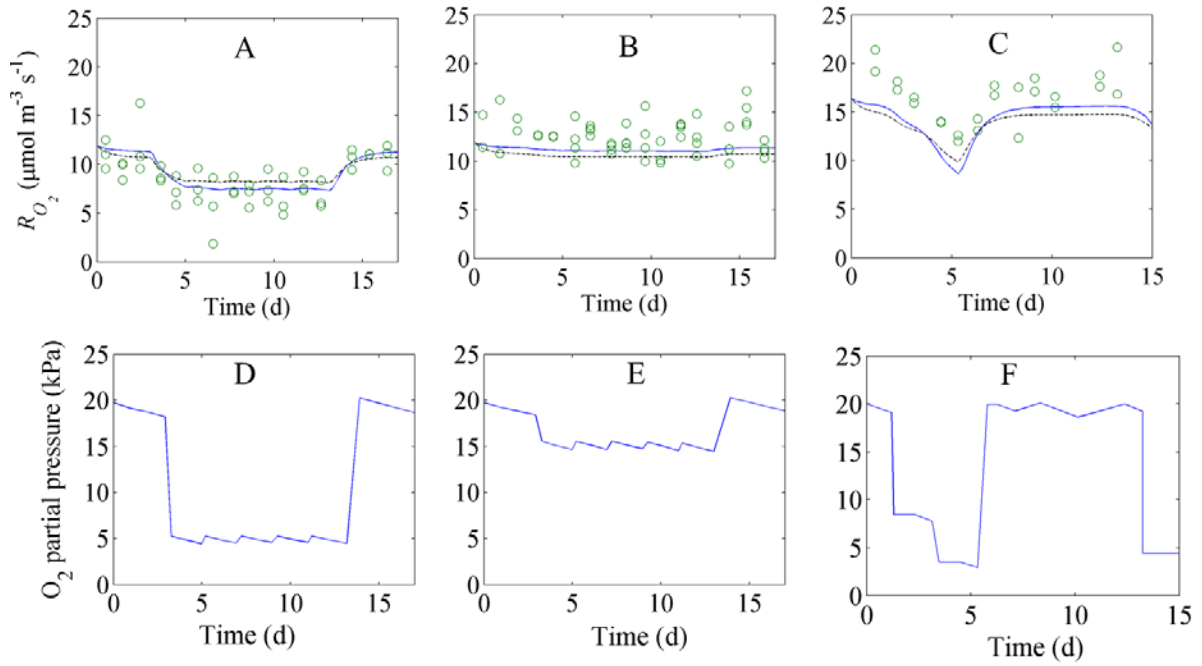


**Fig. S4. Dynamic response of O<sub>2</sub> consumption rate ( $R_{O_2}$ ) to O<sub>2</sub> level and time at 0 °C (experiment B).** Panels (A, B, C) and (D, E, F) are  $R_{O_2}$  and external O<sub>2</sub> level as a function of time, respectively. Symbols (o) indicate measurements while dashed (---) and solid (—) lines show model predictions with  $m$  equal to 1 and 2, respectively.

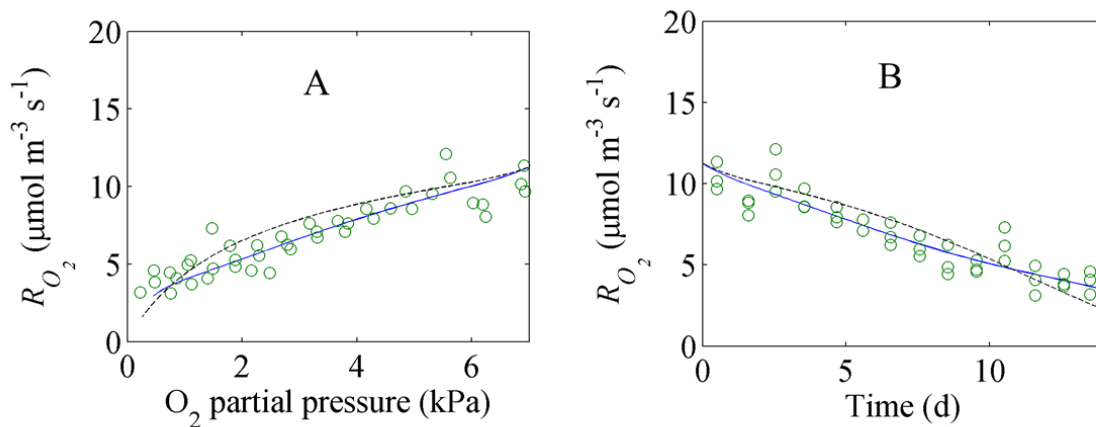


**Fig. S5. Response of  $R_{O_2}$  of intact pear fruit to  $O_2$  (A) and time (B) (experiment C).** Symbols (o) indicate measurements while dashed (— —) and solid (—) lines show model predictions with  $m$  equal to 1 and 2, respectively.

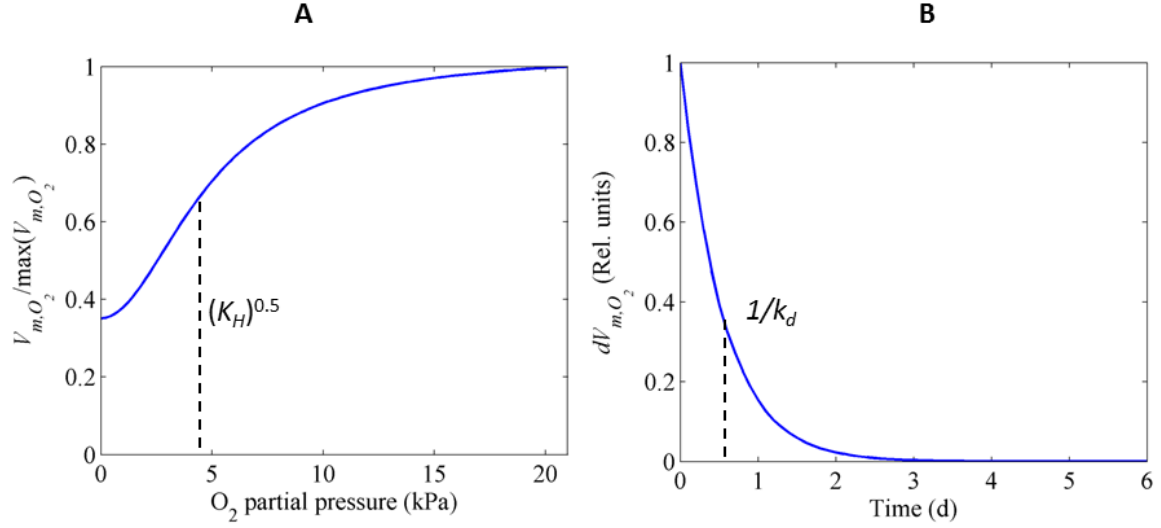


**Fig. S6. (A) Steady state modelled response of relative maximal O<sub>2</sub> consumption rate ( $V_{m,O_2}/\max(V_{m,O_2})$ ) to O<sub>2</sub> level. At a steady state  $V_{m,O_2} = V_R$ . (B) Change of maximal O<sub>2</sub> consumption rate in response to a sudden drop of the O<sub>2</sub> concentration.**

$$dV_{m,O_2} = \frac{V_{m,O_2} - V_R}{V_{m,O_2,ini} - V_R}, \text{ where } V_{m,O_2} \text{ and } V_{m,O_2,ini} \text{ are the maximal O}_2 \text{ consumption rate at time } t \text{ and initial time; } V_R \text{ is the maximal O}_2 \text{ consumption rate at a steady O}_2 \text{ concentration level}$$

(defined in Eq S13).  $k_d$  and  $K_H$  are defined in Eqs S6 and S9, respectively.

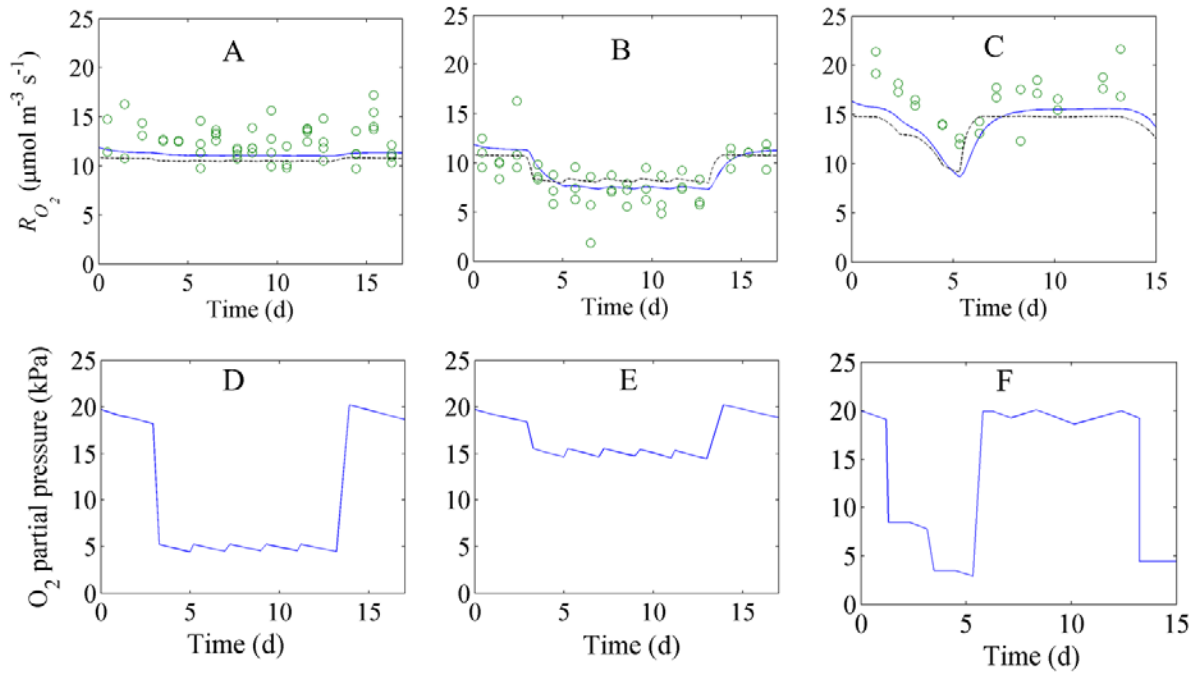


**Fig. S7. Comparison of fitting between the adapted respiration model ( $m = 2$ ) and the respiration model with assumption of variation of  $K_{m,O_2}$  at  $0\text{ }^\circ\text{C}$ .** Panels (A, B, C) and (D, E, F) are  $R_{O_2}$  and external  $O_2$  level as a function of time, respectively. Symbols (o) indicate measurements (experiment B) while dashed (---) and solid (—) lines show model with variation of  $K_{m,O_2}$  and the adapted respiration model, respectively.

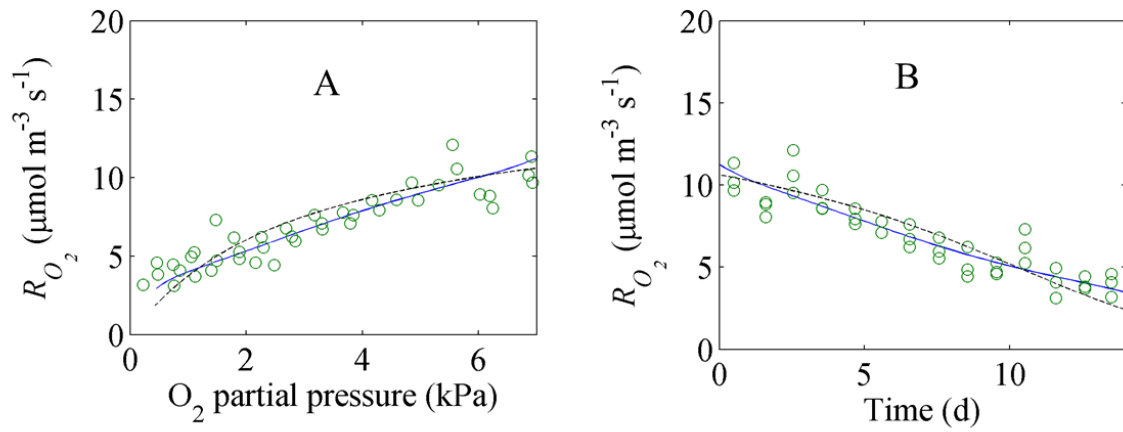


**Fig. S8. Comparison of fitting between the adapted respiration model ( $m = 2$ ) and the respiration model with assumption of variation of  $K_{m,O_2}$  at  $0\text{ }^\circ\text{C}$ .** Symbols (o) indicate measurements (experiment C) while dashed (---) and solid (—) lines show model with variation of  $K_{m,O_2}$  and the adapted respiration model, respectively.

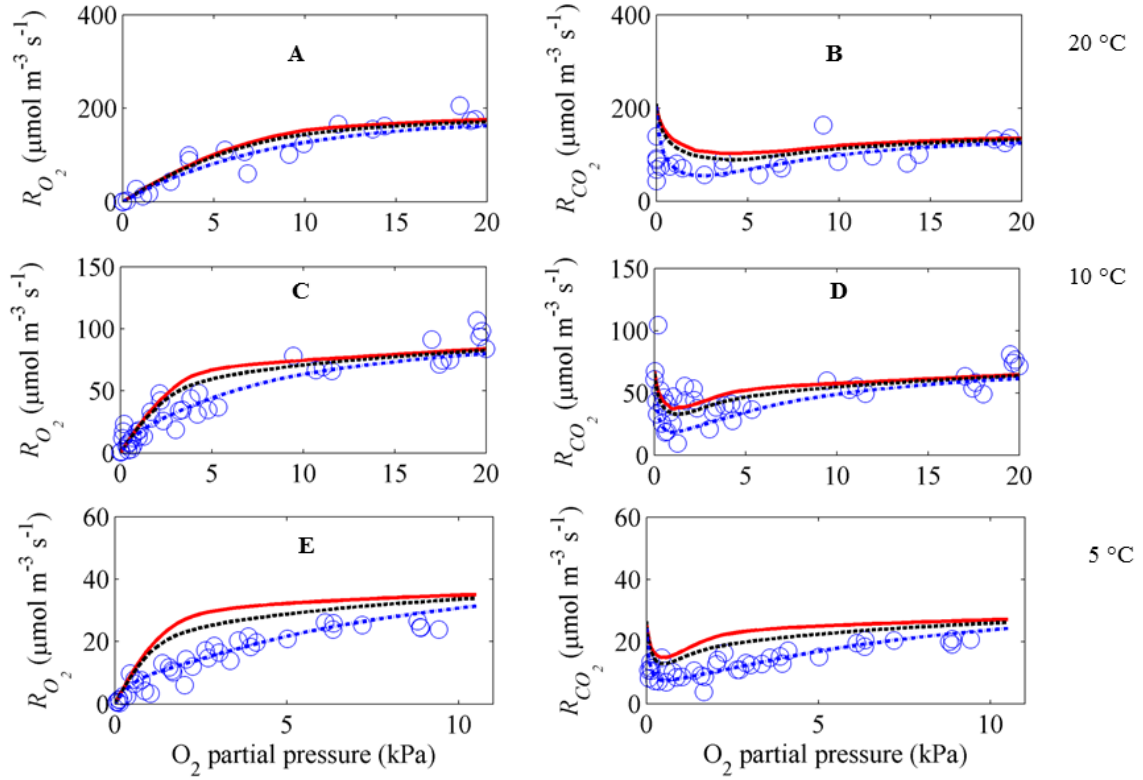


**Fig. S9. Respiration rate of intact pear fruit as a function of the O<sub>2</sub> concentration at 20 °C (A, B), 10 °C (C, D), and 5 °C (E, F) harvested in season 2016.**  $R_{O_2}$  and  $R_{CO_2}$  are the O<sub>2</sub> consumption rate and CO<sub>2</sub> production rate, respectively. Symbols (o) indicate measurements (experiment D). Solid red lines (—), dashed black lines (— —) and dotted blue lines (···) correspond to simulations with assumed  $\frac{\Delta V}{V_{R,2}}$  of 0, 0.21 and 0.66, respectively. Ratio  $\frac{\Delta V}{V_{R,2}}$  represents the amplitude of regulation of maximal respiration rate by O<sub>2</sub> (see in Supplementary text S1 for its derivation). Measurements were carried out in the season of 2016.



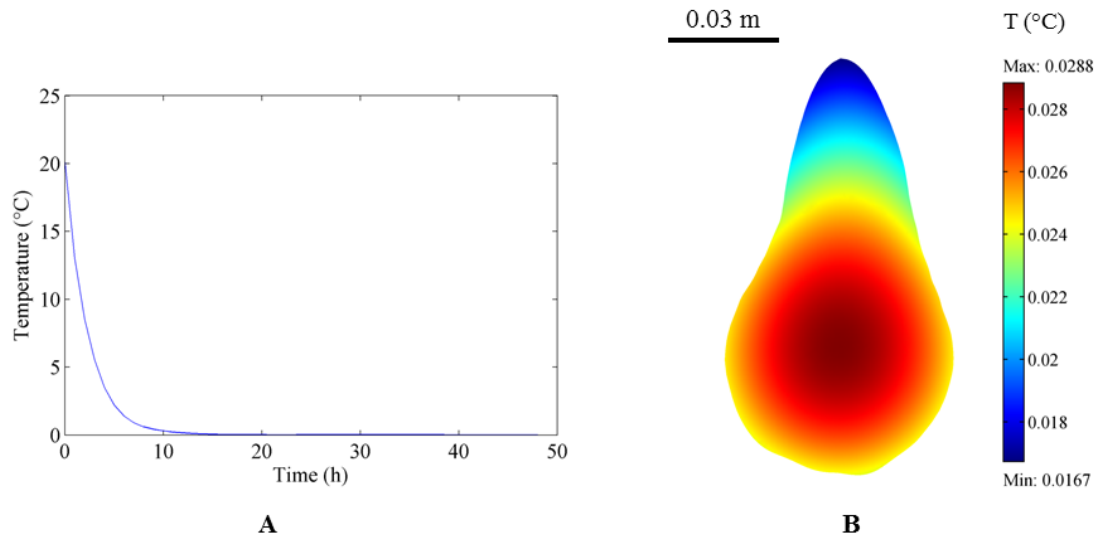


**Fig. S10. Predicted temperature of pear fruit during cooling.** (A) Mean fruit temperature as a function of time during cooling from 20 °C to 0 °C; (B) Temperature profile within the pear at steady state at 0 °C. The maximal temperature difference is about 0.01 °C. The temperature is not completely equal to 0 °C because of the heat production caused by respiration.

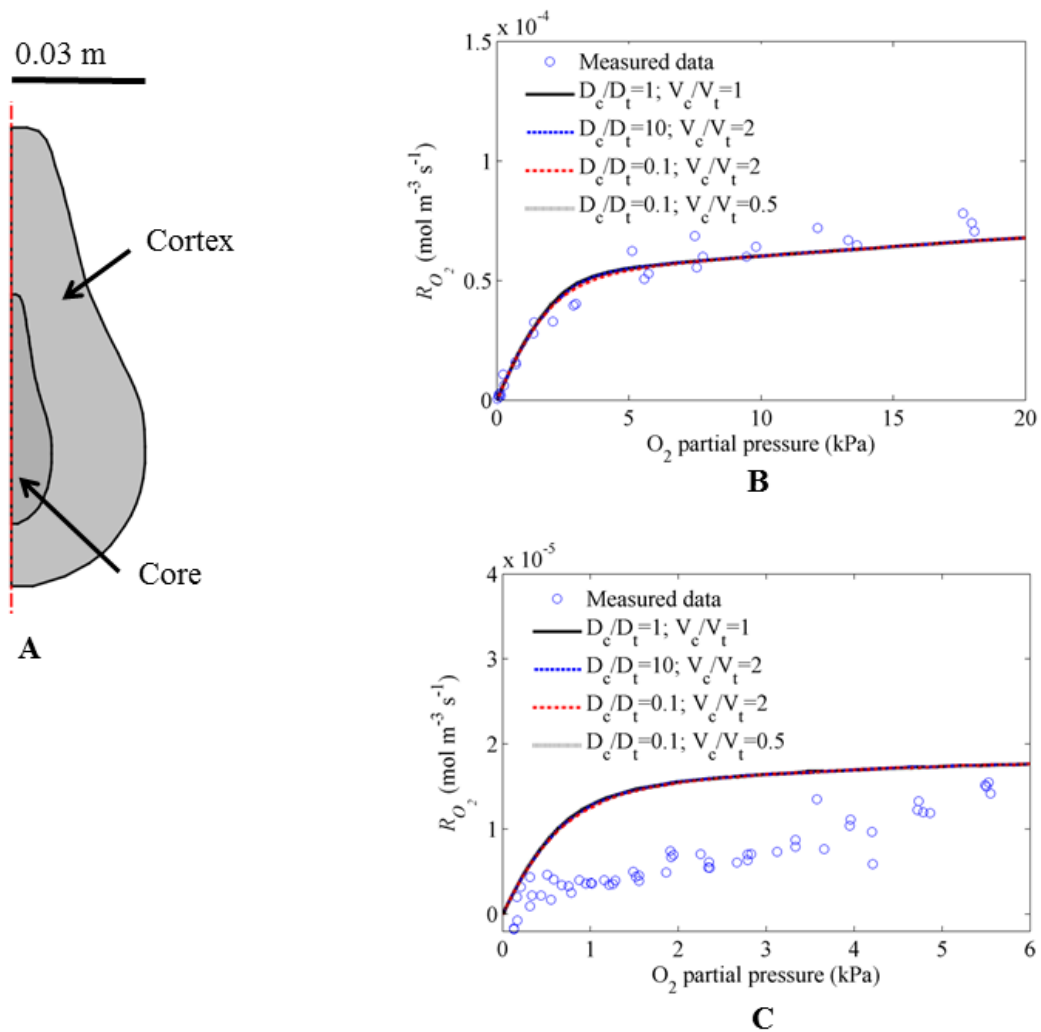


**Fig. S11. Simulations with a two-compartment model (core and cortex) and different combinations of diffusivities and  $V_{max}$  values.** (A) 2D axisymmetric model of the pear fruit. The core was obtained by scaling the fruit to 30% of its origin size. The volume of the core occupied 4.5% of the fruit volume. (B) and (C) show the O<sub>2</sub> consumption rates of intact pear fruit as a function of O<sub>2</sub> concentrations at 10 °C and 0 °C, respectively. Symbols indicate the measured data while lines represent simulations.  $D_c/D_t$  is the ratio of the diffusivity of the core ( $D_c$ ) to that of the cortex ( $D_t$ ) while  $V_c/V_t$  is the ratio of the maximal respiration rate of the core ( $V_c$ ) to that of the cortex ( $V_t$ ). Values of  $D_t$  and  $V_t$  were taken from Table 1 and Table 2, respectively while values of  $D_c$  and  $V_c$  were assumed to vary. Respiration was assumed to follow Michaelis Menten kinetics

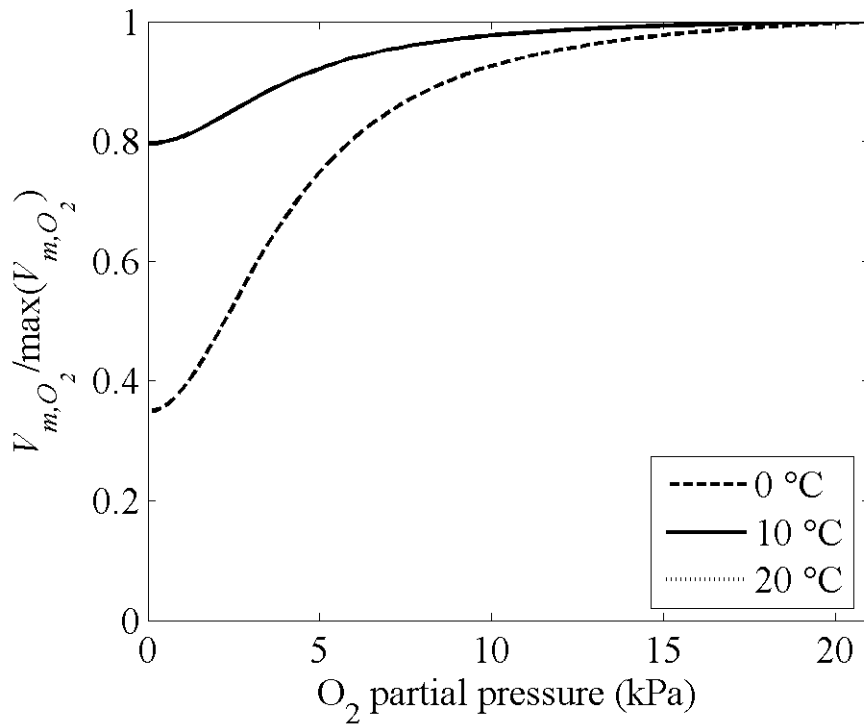


**Fig. S12. Steady state modelled response of relative maximal O<sub>2</sub> consumption rate ( $V_{m,O_2} / \max(V_{m,O_2})$ ) to O<sub>2</sub> level.**  $\Delta V$  which represents response of the maximal respiration rate to O<sub>2</sub> level was assumed to be equal to  $0.66 \cdot V_{R,2}$ ,  $0.21 \cdot V_{R,2}$  and  $0.21 \cdot V_{R,2}$  at 0 °C, 10 °C and 20 °C, respectively. The curve at 10 °C is coincident to that at 20 °C.

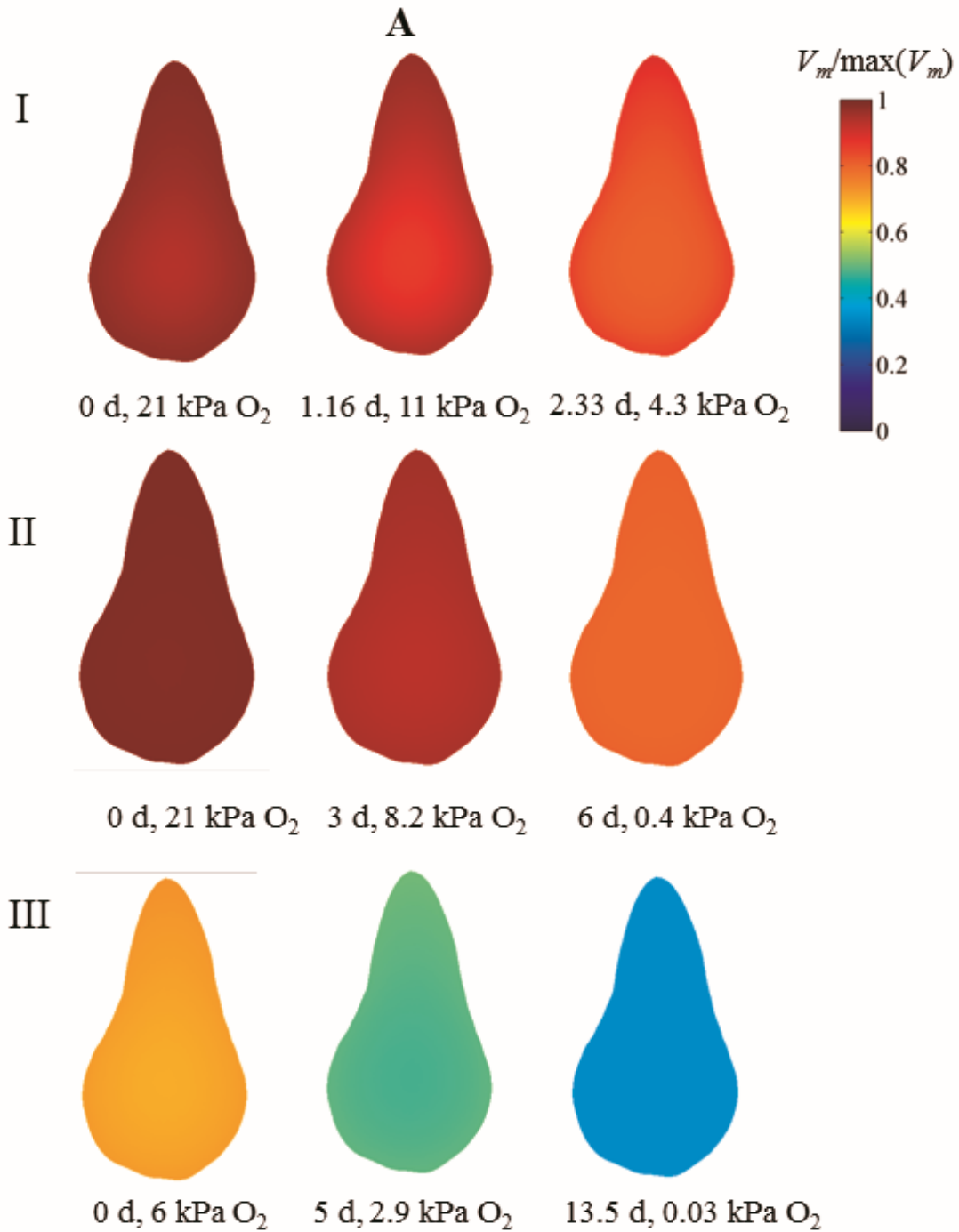


**Fig. S13. Simulated  $V_{m,O_2}$  of pear fruit in the closed jar at 20 °C (I), 10 °C (II) and 0 °C (III) and different times.** The color map represents  $V_{m,O_2} / \max(V_{m,O_2})$ . In the simulations, Ratio  $\Delta V/V_{R,2}$  representing amplitude of regulation of maximal respiration rate by O<sub>2</sub> (see in Supplementary text S1 for its derivation) was assumed to be 0.21, 0.21 and 0.66 at 20 °C, 10 °C and 0 °C, respectively. Simulated  $V_{m,O_2}$  corresponds to O<sub>2</sub> and CO<sub>2</sub> partial pressures of pear fruit described in Fig. 2.

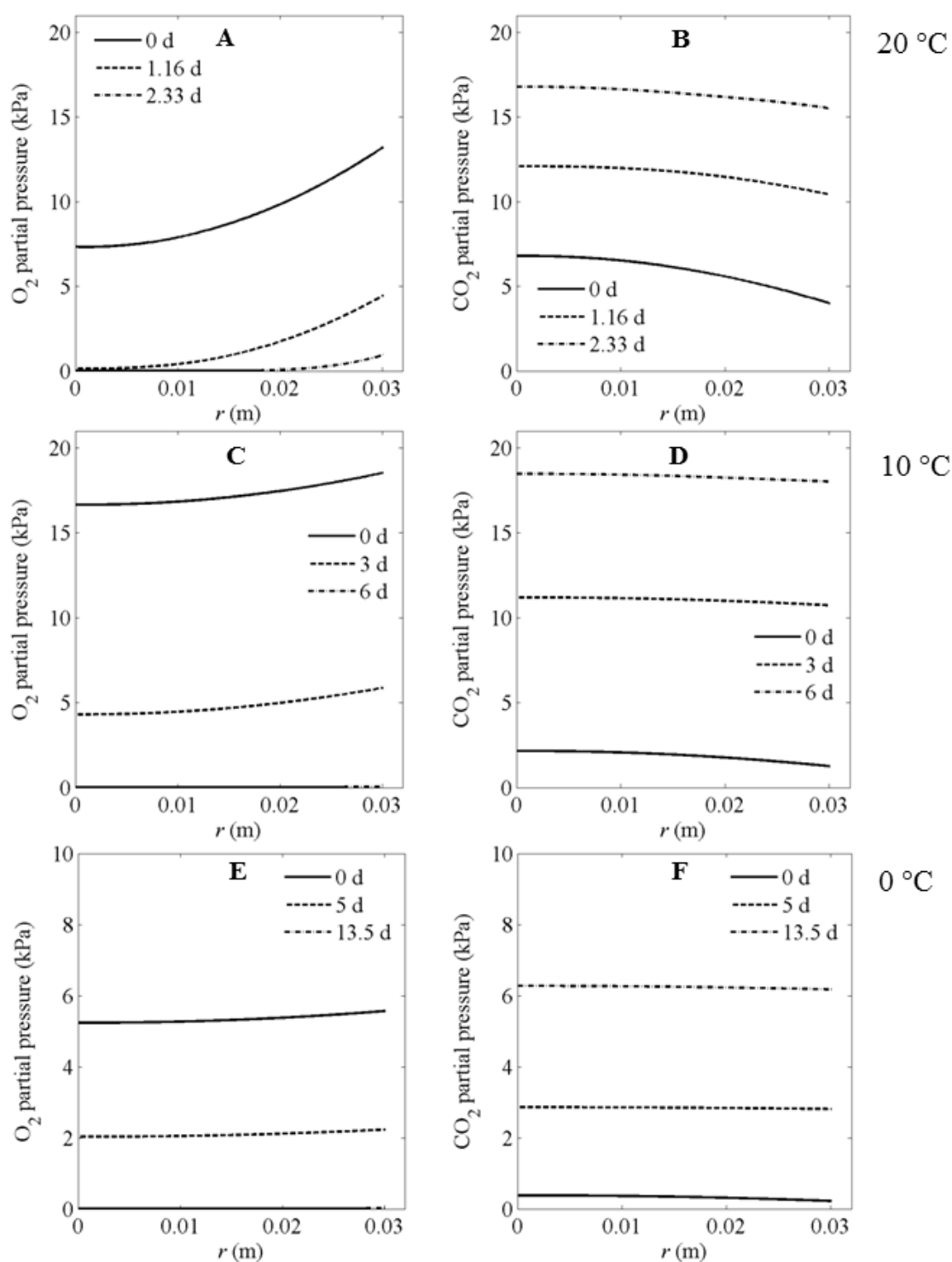


**Fig. S14. Simulated O<sub>2</sub> and CO<sub>2</sub> gas partial pressure profiles from the center to the surface along the radial direction in the closed jar at 20 °C (I), 10 °C (II) and 0 °C (III) at different times (where responses of respiration rate to time and O<sub>2</sub> level were described in Fig.3).**

**References:**

**Hill AV.** 1910. The possible effects of the aggregation of the molecules of hæmoglobin on its dissociation curves. *The Journal of Physiology* **40**, 01-22 (Suppl): iv–vii. *doi:10.1113/jphysiol.1910.sp001386*.

**Ramaswamy HS, Tung MA.** 1981. Thermophysical properties of apples in relation to freezing. *Journal of Food Science* **46**, 724–728.

**Rao MA, Rizvi, SSH, Datta AK.** 2005. *Engineering Properties Of Foods*. CRC Press, New York.